Frequency characteristics of wireless power transfer in seawater via magnetic resonant coupling

Yuki MIYAKOZAWA Takehiro IMURA and Yoichi HORI

Faculty of Science and Technology, Tokyo University of Science 2641 Yamazaki, Noda-shi, Chiba, 278-8510 Japan

Abstract Wireless power transfer in seawater has been a problem due to seawater being a highly conductive medium causing eddy current losses to occur between the transmitter and receiver, making it difficult to obtain stable power efficiency. Therefore, we added a polyethylene sheet between the coil and seawater and verified the improvement of efficiency by increasing the spacer distance. We also revealed the frequency characteristics of the coils depending on the separation distance. These are shown through multiple experiments.

Keyword Underwater Wireless Power Transfer, seawater, Frequency Characteristic

1. INTRODUCTION

Japan has the world's sixth largest Exclusive Economic Zone, and the existence of many resources such as oil, natural gas, methane hydrate and seafloor hydrothermal deposits have been confirmed in the surrounding waters. In order to exploit and supply these resources, it is essential to construct an efficient seafloor mapping and exploration system. This is why autonomous underwater vehicle (AUVs) have been developed in recent years. Currently, AUVs have limited operating time due to the limitations of their internal batteries. In addition, when recharging the battery, the AUVs must be brought up to the water's surface and lifted by a crane ships, which requires time and effort. As a solution to this problem, wireless power transfer in seawater has been proposed [1]-[3]. As shown in Fig. 1, a power supply spot is set up in the seawater and AUVs can actively supply power for long hours of operation. However, because seawater is highly conductive, eddy current losses occur in seawater, making it difficult to obtain stable power efficiency [4][5]. Since the optimal frequency band for wireless power transfer in seawater is unclear, changes in frequency characteristics due to it will be revealed in this paper. We will also compare and reveal the characteristics from the analysis and the experiment, when spacers are placed between the coil and seawater.

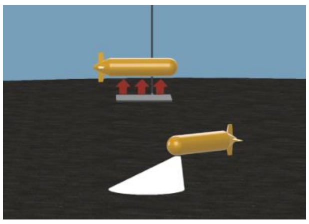

Fig. 1 Image of Underwater wireless power transfer

2. CHANGE IN COIL CHARACTERISTICS DUE TO SEAWATER

2.1 EQUIVALENT CIRCUIT OF COIL WITH EDDY CURRENT LOSS

Seawater is a medium with high conductivity, and the presence of seawater near the coil causes eddy currents in the seawater as shown in Fig. 2, which deteriorates the coil characteristics. A diagram showing the circuit for Fig. 2 is shown in Fig. 3 (a), and the T-type equivalent circuit of Fig. 3 (a) is shown in Fig. 3 (b) [6].

From Kirchhoff's law, equation (1) is obtained.

$$\begin{pmatrix} V \\ 0 \end{pmatrix} = \begin{pmatrix} j\omega(L_{coil} + L_m) + R_{coil} & -j\omega L_m \\ -j\omega L_m & j\omega(L_{eddy} + L_m) + R_{eddy} \end{pmatrix} \begin{pmatrix} I_{coil} \\ I_{eddy} \end{pmatrix} \quad (1)$$

Next, the synthetic impedance Z_{all} is derived and shown in equation (2).

$$Z_{all} = R_{coil} + j\omega L_{coil} + \frac{\omega^2 L_m^2 R_{eddy} - j\omega\{\omega^2 L_{eddy}(L_{eddy} + L_m) + R_{eddy}^2\}}{R_{eddy}^2 + \omega^2 L_{eddy}^2} \quad (2)$$

From equation (2), the equivalent internal resistance R_{all} of the coil in seawater is expressed as in equation (3).

$$R_{all} = R_{coil} + \frac{\omega^2 {L_m}^2 R_{eddy}}{R_{eddy}^2 + \omega^2 L_{eddy}^2} \quad (3)$$

From equation (3), equivalent internal resistance R_{all} of the coil in seawater expressed as a function of ω. From equations (2) and (3), the Q value of the coil in seawater is shown in equation (4).

$$Q = \frac{\omega\{R_{eddy}^2(L_{coil} - 1) + \omega^2 L_{eddy}(L_{coil}L_{eddy} - L_{eddy} - L_m)\}}{R_{coil}(R_{eddy}^2 + \omega^2 L_m^2) + \omega^2 L_m^2 + R_{eddy}} \quad (4)$$

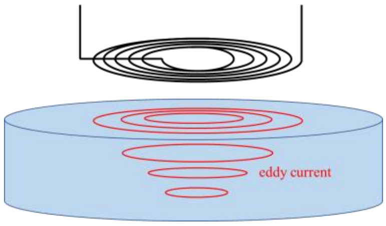

Fig. 2 Model of coil with eddy current

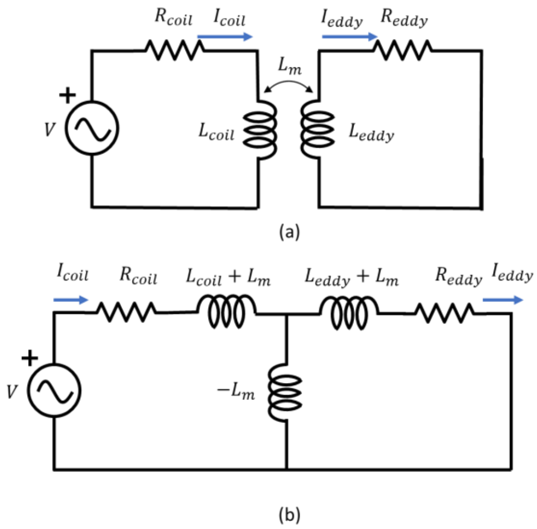

Fig. 3 Equivalent circuit of coil with eddy current loss

2.2. VERIFICATION BY SIMULATION

Next, the equivalent circuit and equations obtained in 2.1 are verified by analysis and experiment. First, the verification is performed by electromagnetic field analysis using the method of moments. The coil used in the analysis is 350 mm × 350 mm on the outside, with 10 turns and a wire diameter of 3 mm. The model used in the analysis is shown in Fig. 4.

The seawater volume is 700 × 700 × 300 mm, the transmission distance is 100 mm, and a seawater model is created with a 0.2 mm space between the coil and seawater to prevent seawater from conducting current. Table. 1 shows the parameters used in the simulation. ε_r is the relative permittivity, μ_r is the relative permeability and σ is the conductivity. A graph of the frequency characteristics of the inductance L and coupling coefficient k of the coil in seawater obtained from the analysis is shown in Fig. 6, Fig. 7 shows a graph of the maximum efficiency η_{max} derived from the analytical results using equation (5) [7]. The measured values of the graphs are shown in the next section 2.3.

$$\eta_{max} = \frac{k^2 Q^2}{\left(1+\sqrt{1+k^2Q^2}\right)^2}. \quad (5)$$

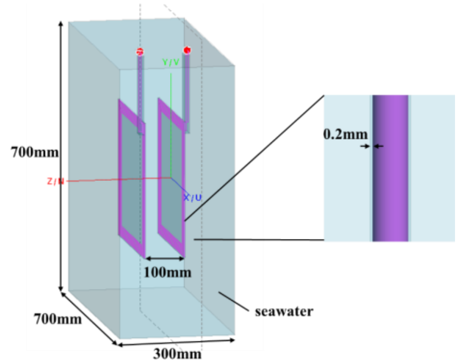

Fig. 4 Simulation model for underwater coils

Table. 1. simulation parameters

	ε_r	μ_r	σ $[S/m]$	specific gravity $[kg/m\text{^}3]$
Seawater	78	1	5.3	1020

2.3. VERIFICATION BY EXPERIMENT

Nexct, the frequency characteristics of an actual tank (700 × 700 × 800 mm) filled with artificial seawater are measured. For the measurement, a coil of the same size as that used in the analysis was created, and the measurement was performed using a impedance analyzers. The actual experiment is shown in Fig. 5.

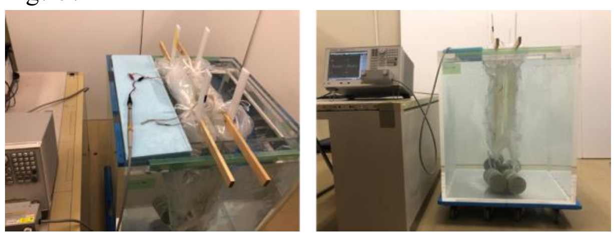

Fig. 5 Measurement setup for underwater coils

The results of the frequency response of the inductance L and coupling coefficient k obtained from the measurement and analysis are shown in Fig. 6. Fig. 7 shows a graph of the maximum efficiency η_{max} derived from equation (5) using the results obtained from Fig. 6. The analytical and experimental results show that the internal resistance of the coil in seawater increases in proportion to the frequency, and the Q value decreases significantly due to this effect. As shown in Table 2, the maximum Q value Q_{max} was 565 at 208.8 kHz in air, while it was 115 at 34.1 kHz in seawater. The coupling coefficient does not change significantly, and Fig. 7 shows that the maximum efficiency η_{max} also decreases as the Q value decreases.

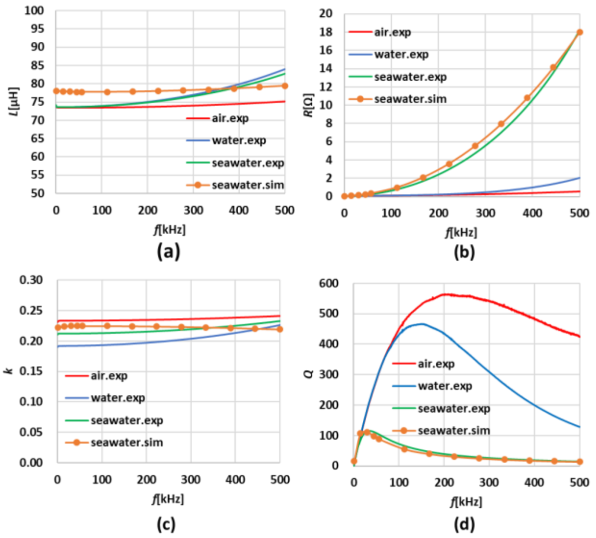

Fig. 6 Simulation and measurement results of frequency characteristics of underwater coils (a)Inductance (b)Resistance (c)Coupling coefficient (d)$\boldsymbol{Q}$

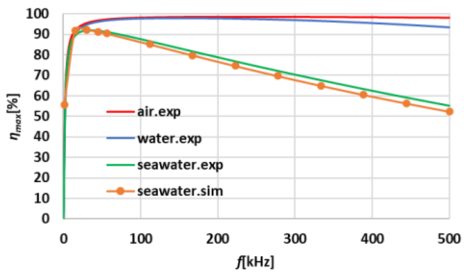

Fig. 7 Simulation and measurement results of maximum frequency of underwater coils

Table. 2 Maximum Q value of coil

	f [kHz]	Q_{max}	η_{max} [%]
Air	208.8	565.0	99.1
Water	150.0	465.8	98.5
Seawater	34.1	115.0	93.6

3. CHANGE IN CHARACTERISTICS WITH SPACER

3.1. VERIFICATION BY SIMULATION

Next, the change in coil characteristics when spacing is added between the coils and seawater between the transmitter and receiver is verified by analysis and experiment. The coil geometry and model used in the analysis are the same as in the previous section 2.2. From there, free space are placed between the coil and seawater. The width of the spacer is s and analysis is performed for $s = 0, 5, 10, 20, 30, 40$ and 50 mm, respectively, for comparison. At $s = 50$mm all the space between the transmitter and receiver is free space. The results of the analysis are shown in Fig. 9 and Fig. 10.

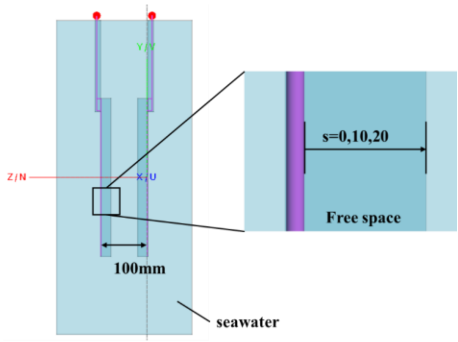

Fig. 8 Simulation model for underwater coils with inserting spacer between seawater and coil

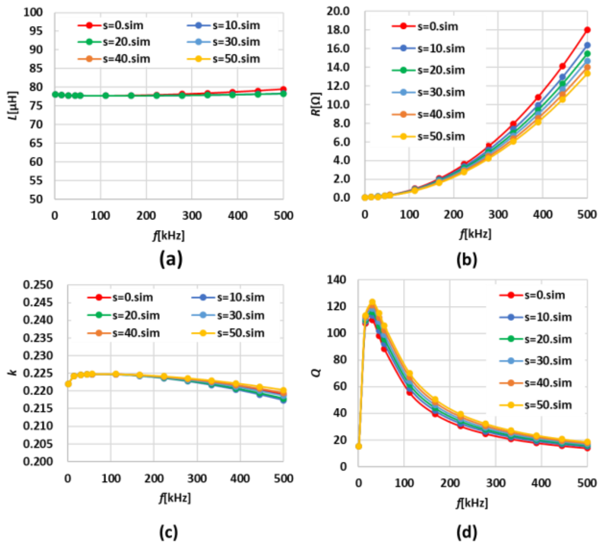

Fig. 9 Simulation results of frequency characteristics of underwater coils with spacer (a)Inductance (b)Resistance (c)Coupling coefficient (d) Q

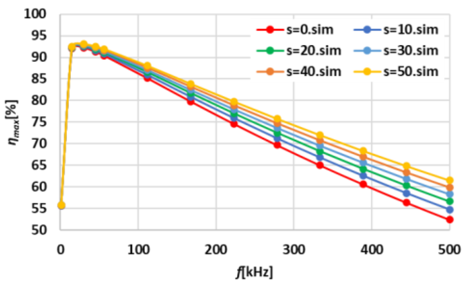

Fig. 10 Simulation results of maximum frequency of underwater coils with spacer

3.2. VERIFICATION BY EXPERIMENT

The following are the results of the experiment. Foamed polyethylene was attached as a spacer to the coil, and measurements were taken at $s = 0, 5$, and 10 mm, respectively, as in the analysis. The measured results are shown in Fig. 9 and Fig. 10.

Fig. 9 and Fig. 10 show that inductance L and internal resistance R vary with the spacer, and that the larger the width of spacer s, the higher the Q value of the coil. However, there is almost no change in the coupling coefficient k even when there is no seawater between the transmitter and receiver, indicating that the main cause of the lower efficiency of wireless power transfer in seawater is the deterioration of the characteristics of the coil itself rather than the attenuation of the magnetic field in seawater. The maximum efficiency η_{max} increased by 1.3% for $s = 0$mm and $s = 50$mm at 45 kHz, while it increased by 9.1% at 500 kHz, indicating that the improvement in coil characteristics by the spacer is greater at higher frequencies.

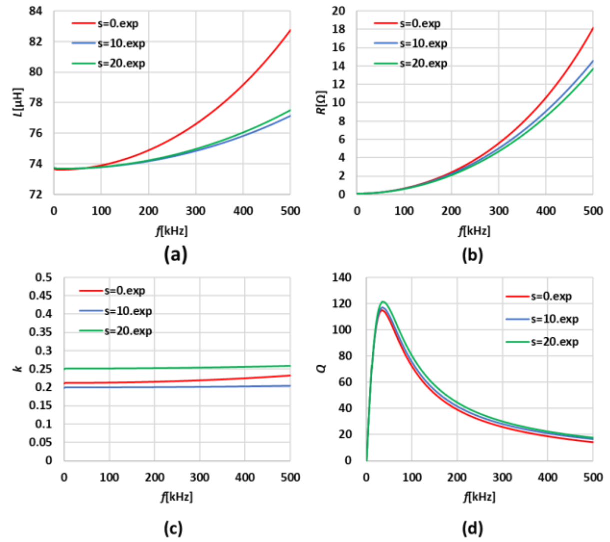

Fig. 11 Measurement results of frequency characteristics of underwater coils with spacer (a)Inductance (b)Resistance (c)Coupling coefficient (d)Q

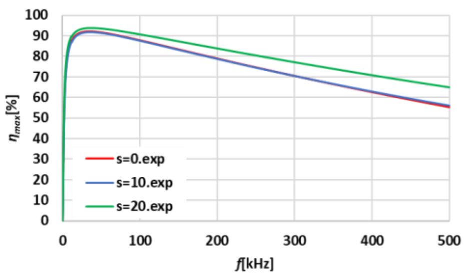

Fig. 12 Measurement results of maximum frequency of underwater coils with spacer

4. Conclusion

Analyses and experiments were conducted on the characteristics of coils in air, water, and seawater media, respectively, to compare and reveal the changes in frequency characteristics. It can be seen that the internal resistance of the coil in seawater increases in proportion to the frequency, and the Q value decreases significantly due to this effect. Although the characteristics of the coil itself used in this study are also relevant, it had a Q_{max} of 115 at 34.1 kHz in seawater, resulting in a maximum efficiency of 93.6%. It was also found that the coupling coefficient did not change significantly and the maximum efficiency η_{max} also decreased as the Q value decreased. Next, the changes in coil characteristics by inserting spacers ($s = 0, 10, 20$ mm) between the coil and seawater were compared and verified through analyses and experiments. It was found that the main reason for the efficiency decreasing in seawater was the deterioration of coil characteristics, and that the spacers improved the Q value of the coil, with the higher frequency having a greater effect with the spacers.

5. References

[1] R. Hasaba, K. Eguchi, S. Yamaguchi, H. Satoh, T. Yagi and Y. Koyanagi, "WPT System in Seawater for AUVs with kW-class Power, High Positional Freedom, and High Efficiency inside the Transfer Coils," 2022 Wireless Power Week (WPW), 2022, pp. 90-94.

[2] J. Zhou, P. Yao, Y. Chen, K. Guo, S. Hu and H. Sun, "Design Considerations for a Self-Latching Coupling Structure of Inductive Power Transfer for Autonomous Underwater Vehicle," in IEEE Transactions on Industry Applications, vol. 57, no. 1, pp. 580-587, Jan.-Feb. 2021.

[3] T. Kan, R. Mai, P. P. Mercier and C. C. Mi, "Design and Analysis of a Three-Phase Wireless Charging System for Lightweight Autonomous Underwater Vehicles," in IEEE Transactions on Power Electronics, vol. 33, no. 8, pp. 6622-6632, Aug. 2018.

[4] Z. Liu, L. Wang, Y. Guo and C. Tao, "Eddy Current Loss Analysis of Wireless Power Transfer System for Autonomous Underwater Vehicles," 2020 IEEE PELS Workshop on Emerging Technologies: Wireless Power Transfer (WoW), 2020, pp. 283-287.

[5] K. Zhang, Y. Ma, Z. Yan, Z. Di, B. Song and A. P. Hu, "Eddy Current Loss and Detuning Effect of Seawater on Wireless Power Transfer," in IEEE Journal of Emerging and Selected Topics in Power Electronics, vol. 8, no. 1, pp. 909-917, March 2020.

[6] Khokle, Rajas Prakash, Karu P. Esselle, and Desmond J. Bokor. 2018. "Design, Modeling, and Evaluation of the Eddy Current Sensor Deeply Implanted in the Human Body" *Sensors* 18, no. 11: 3888.

[7] K. Hata, T. Imura and Y. Hori, "Simplified measuring method of kQ product for wireless power transfer via magnetic resonance coupling based on input impedance measurement," *IECON 2017 - 43rd Annual Conference of the IEEE Industrial Electronics Society*, 2017, pp. 6974-6979.